Inorganica Chimica Acta 528 (2021) 120590

Contents lists available at ScienceDirect

Inorganica Chimica Acta

journal homepage: www.elsevier.com/locate/ica

Research paper

Biologically active acylthioureas and their Ni(II) and Cu(II) Complexes: Structural, spectroscopic, anti-proliferative, nucleolytic and antimicrobial studies

Ebube E. Oyeka [a,b], Ilknur Babahan [c], Bernard Eboma [a], Kenechukwu J. Ifeanyieze [a], Obinna C. Okpareke [a,*], Esin P. Coban [d], Ali Özmen [d], Burak Coban [e], Mehran Aksel [f], Namık Özdemir [g], Tatiana.V. Groutso [h], Jude I. Ayogu [a], Ufuk Yildiz [e], Mehmet Dinçer Bilgin [f], H. Halil Biyik [d], Briana R. Schrage [i], Christopher J. Ziegler [i], Jonnie N. Asegbeloyin [a,*]

[a] Department of Pure and Industrial Chemistry, University of Nigeria, Nsukka, Enugu State, Nigeria
[b] Department of Chemistry, Clemson University, Clemson, SC 29634, USA
[c] Department of Chemistry, Aydin Adnan Menderes University, 09010 Aydin, Turkey
[d] Department of Biology, Aydin Adnan Menderes University, 09010 Aydin, Turkey
[e] Department of Chemistry, Zonguldak Bulent Ecevit University, 67100 Zonguldak, Turkey
[f] Department of Biophysics, Faculty of Medicine, Aydin Adnan Menderes University, 09010 Aydin, Turkey
[g] Department of Mathematics and Science Education, Faculty of Education, Ondokuz Mayıs University, 55139 Samsun, Turkey
[h] School of Chemical Sciences, The University of Auckland, New Zealand
[i] Department of Chemistry, University of Akron, Akron, OH 44325, USA

ARTICLE INFO

Keywords:
Anticancer
Antimicrobial
Complexes
DNA binding
Morpholine
Thiourea
X-ray diffraction
Breast cancer (MCF-7)
Prostate cancer (PC-3)

ABSTRACT

The study investigated the effects of morpholine substituent and metal complexation on *in vitro* anticancer and antimicrobial activities of acylthioureas using two acylthiourea molecules that differ only by the presence of morpholine oxygen; *N,N*-diethyl-N′-(4-chlorobenzoyl)thiourea (*CBDEA*) and *N*-morpholine-*N*′-(4-chlorobenzoyl) thiourea (*CBMOR*), and their Ni(II) and Cu(II) complexes (*NiCBDEA, CuCBDEA, NiCBMOR, CuCBMOR*). All compounds were synthesized and characterized by physicochemical and spectroscopic studies. *CBDEA, CuCBDEA, NiCBDEA, CBMOR,* and *NiCBMOR* were structurally elucidated by single-crystal X-ray diffraction. The metal complexes were isolated as neutral four coordinate complexes of the form, ML_2 (M: Ni(II), Cu(II), H.L.: *CBDEA/CBMOR*) in square-planar geometry. The compounds were screened for DNA binding/cleavage, antimicrobial activity, and anti-proliferative effects on human prostate cancer PC-3 and breast cancer MCF-7 cells. DNA binding interaction studies suggest that the metal complexes bind more strongly to the DNA compared to the ligands. The morpholine derivative *CBMOR* shows similar activity to *CBDEA* against PC-3 cell lines but twice as effective against MCF-3 cells at cell death and apoptotic levels. Anticancer activities were enhanced by complexation with Cu(II), as evident in *CuCBMOR,* which showed the optimal anticancer activity (IC50: 1.76 μM for MCF-7 and 1.97 μM for PC-3), comparable to known anticancer drug *paclitaxel*. The *CuCBMOR* apoptosis results show that the cancer cells die by apoptotic mechanisms (Apoptosis rate: 91.53 % in MCF-7 and 85.95 % in PC-3). In vitro screening of the compounds against seventeen bacteria and four yeast strains confirmed antimicrobial potency against more susceptible Gram-positive bacteria strains. The results of the study suggest that some of the compounds could be developed into novel antimicrobial and anticancer agents.

1. Introduction

Breast cancer is the most frequent malignant cancer among women, and the second most common cancer worldwide, while prostate cancer is only second to lung cancer among other frequent tumors found in men [1,2]. For decades, several platinum-based drugs have played front-line roles in the treatment of different forms of cancer; however, some limitations such as adverse side effects of most anticancer drugs and low

* Corresponding authors.
E-mail addresses: obinna.okpareke@unn.edu.ng (O.C. Okpareke), niyi.asegbeloyin@unn.edu.ng (J.N. Asegbeloyin).

https://doi.org/10.1016/j.ica.2021.120590
Received 31 May 2021; Received in revised form 22 August 2021; Accepted 23 August 2021
Available online 27 August 2021

clinical efficacy still necessitate a constant search for new drugs. One approach to a more synergistic anticancer agent is to develop metal complexes with biologically friendly metals that can mimic the chemistry of Pt(II), such as in the formation of square-planar geometry and soft Lewis acidity [3,4]. Cu(II) and Ni(II) fit well into this category because of their vast enzymatic activities, tendency to coordinate in square-planar geometry, and ability to form stable compounds with ligands containing hard O- and N- donor atoms and soft S- donor atom such as thioureas, and acylthioureas [5,6].

Literature survey has revealed that thioureas are an excellent pool of bioactive moieties, with activities such as anticancer [7,8], antimicrobial [9,10], analgesic [11], antituberculosis [12], and anti-HIV [13]. Compared to thioureas, acylthioureas have increased coordination possibility because of the presence of the carbonyl oxygen. The blend and orientation of the hard O- and soft S- donor atoms in the acylthiourea backbone enable them to bond readily to Ni(II) and Cu(II) ions in a square-planar fashion. Several stable metal complexes of acylthioureas with interesting physicochemical properties and significant biological activity have been reported [10-14]. Among the acylthiourea compounds, benzoylthioureas have been well studied as bioactive agents [14,15]. However, the effect of bioactive substituents has only been mildly explored. To bridge this gap, we investigate the effect of morpholine in the biological potency of benzoylthioureas and their Ni(II) and Cu(II) complexes. Morpholine is a known bioactive substituent with activity including antimicrobial, HIV-protease inhibition, antituberculosis, antitumor, and human neurokinin-1 (hNK-1) receptor antagonism [7,16,17]. The addition of the morpholine group to ibuprofen and indomethacin has been reported to lead to increased selective COX-2 inhibitory activity [18]. Recently, ongoing research on morpholine-directed targeted therapy was reported [19]. This has further aroused our interest in investigating morpholine-based anticancer drugs. *N,N*-diethyl-*N′*-(4-chlorobenzoyl)thiourea (*CBDEA*) and its morpholine analogue *N*-morpholine-*N′*-(4-chlorobenzoyl)thiourea (*CBMOR*), and their Ni (II) and Cu(II) were synthesized for a comparative anticancer and antimicrobial study. In contrast with previous reports on the spectroscopic and biological studies of *CBDEA* and its Pt(II) complex [20], we present the crystal structures of *CBDEA, CBMOR*, *NiCBDEA, CuCBDEA*, and *NiCBMOR*. All the compounds were screened for DNA cleavage/binding and their antimicrobial potency against seventeen bacteria and four fungi strains. The anti-proliferative effects of these compounds on human prostate cancer PC-3 cells and breast cancer MCF-7 cells were also investigated.

2. Experimental methods

2.1. Chemicals and instrumentation

4-Chlorobenzoylchloride, morpholine, diethylamine, acetone, methanol, dichloromethane, and potassium thiocyanate were obtained from Sigma Aldrich and used without further purification. The melting points were determined with a Fisher John melting point apparatus. The infrared spectra were recorded in the range of 4000 – 400 cm^{-1} as KBr discs on a Perkin Elmer 100 Infrared Spectrophotometer. ^{1}H NMR spectra were obtained from a MERCURY-300 MHz NMR spectrometer using DMSO-D_6 as a solvent. Elemental analyses of C, H, and N, were performed using a Carlo Erba Elemental analyzer EA1108. The conductivity of the complexes was checked using a WTW LF90 conductivity meter. UV–Vis spectra of the synthesized compounds were acquired using a UV-2500PC Series model spectrophotometer. U.V–Vis spectra for DNA titrations were recorded at room temperature on a Cary 100 Bio U. V-Vis spectrophotometer. Solutions of calf thymus DNA (CT-DNA; Sigma D1501) in 100 mM KCl, 10 mM Tris-HCl, and pH-7.5 buffer had a U.V.–Vis absorbance ratio of 1.8 – 1.9: 1 at 260 and 280 nm ($A_{260}/A_{280} = 1.9$), indicating that the DNA was sufficiently free of protein [21]. The concentration of DNA was determined spectrophotometrically using a molar absorptivity of 6600 M^{-1} cm^{-1} (260 nm) [21]. Double-distilled water was used to prepare the buffers. The stock solution of CT-DNA was stored at 4 °C and used within 4 days.

2.2. General procedure for the synthesis of ligands

Synthesis of the ligands was done by using similar literature procedures [22,23]. A solution of 4-chlorobenzoylchloride (0.02 mol) in anhydrous acetone (40 mL) was added dropwise to a suspension of potassium thiocyanate (0.02 mol) in anhydrous acetone (30 mL), and the reaction mixture was heated under reflux for 30 min and then cooled to room temperature. A solution of diethylamine (0.01 mol) or morpholine (0.01 mol) in anhydrous acetone (30 mL) was added, and the resulting mixture was stirred for 2 h at room temperature. The reaction mixture was filtered to remove suspended inorganic solids. The filtrate was left for few days, and colorless solids of *N,N*-diethyl-*N′*-4-chlorobenzoylthiourea (*CBDEA*), or *N*-morpholine-*N′*-4-chlorobenzoylthiourea (*CBMOR*) were obtained (Scheme 1). The solid products were then washed with water and ethanol and dried in the air. Crystals suitable for X-ray crystallographic studies were obtained by slow evaporation of a solution of the compounds in a methanol/dichloromethane (1:1) mixture at room temperature for 7 days.

2.2.1. N,N-diethyl-N′-4-chlorobenzoylthiourea (CBDEA)

Color: colorless; m.p: 156 – 158 °C, yield: 89 %; $C_{12}H_{15}ClN_2OS$ Calculated %: C 53.23, H 5.58, N 10.35 ; Found %: C 53.77, H 5.12, N 10.11; ^{1}H NMR (300 MHz, DMSO D_6) δ: 10.62 (s, 1H, NH), 7.82 – 7.90 (*m*, 2H, Ar-H), 7.46 – 7.54 (*m*, 2H, Ar-H), 3.83 – 3.93 (q, 2H, CH_2-CH_3), 3.44 – 3.50 (q, 2H, -CH_2-CH_3), 1.20 (t, 3H, CH_3-CH_2-, *J* 7.53, 2.26 Hz), 1.14 (t, 3H, CH_3-CH_2-, *J* 7.53, 3.81 Hz); ^{13}C NMR (300 MHz, $CDCl_3$) δ: 179.06 (C═O), 162.89 (C═S), 139.27(C-Cl), 131.00 (C_{para}–Ph), 129.31, 129.07 (C_{meta}–Ph), 128.86, 128.77 (C_{ortho}–Ph), 47.93, 47.68 (CH_2), 11.46, 13.28 (CH_3); IR (KBr): υ(cm^{-1}): 3271 (st, υN-H), 1642 (st, υC = O), 1228 (υC = S). UV: 281 nm (C═S, n π*).

2.2.2. N-morpholine-N′-4-chlorobenzoylthiourea (CBMOR)

Color: colorless; m.p: 146 – 148 °C, yield: 91 %, $C_{12}H_{13}ClN_2O_2S$ Calculated %: C 50.61, H 4.60, N 9.84; Found %: C 51.02, H 4.61, N 9.80; ^{1}H NMR (300 MHz, DMSO D_6): δ = 10.92 (s, 1H, NH), 7.92 – 7.95 (d, 2H, Ar-H), 7.56 – 7.59 (d, 2H, Ar-H), 4.15 (t, 2H, CH_2-CH_2), 3.57 – 3.71 (t, 6H, -CH_2-CH_2); ^{13}C NMR (300 MHz, $CDCl_3$) δ: 178.91 (C═O), 162.31 (C═S), 139.64 (C-Cl), 130.57 (C_{para}–Ph), 129.26 (C_{meta}–Ph), 129.23 (C_{ortho}–Ph), 52.47, 51.60 (CH_2); IR (KBr): υ(cm^{-1}): 3258 (st, υN-H), 1686 (st, υC = O), 1246 (υC = S).; UV: 275 nm (C═S, $n \rightarrow \pi^*$).

2.3. General procedure for the synthesis of metal complexes

A solution of $Ni(CH_3COO)_2{\cdot}4H_2O$ or $Cu(CH_3COO)_2{\cdot}4H_2O$ (1 mmol) in ethanol (20 mL) was added dropwise to a solution of *CBDEA* or *CBMOR* (2 mmol) in dichloromethane in a 1:2 ratio at room temperature. The resulting mixture was refluxed for 30 min at room temperature, and the solid obtained was filtered (Schemes 2a-b). *NiCBDEA* and *CuCBDEA* crystals suitable for X-ray crystallography were obtained by slow evaporation from a 1:1 methanol-dichloromethane solution of the complexes at room temperature for 48 h. *NiCBMOR* crystals were obtained by slow diffusion of ether into dichloromethane solution of the metal complex for a week.

2.3.1. bis(N,N-diethyl-N′-4-chlorobenzoylthioureato)nickel(II) (NiCBDEA)

Colour: red crystals; m.p: 222 °C, yield: 75 %; $C_{24}H_{28}Cl_2N_4NiO_2S_2$; Calculated %: C 48.18, H 4.72, N 9.37; Found %: C 47.98, H 4.72, N 9.41; ^{1}H NMR (300 MHz, DMSO D_6): 8.50 (d, 2H, Ar-H), 8.06 (d, 2H, Ar-H), 4.89 (q, 2H, CH_2-CH_3), 4.39 (q, 2H, -CH_2-CH_3), 1.32–1.40 (t, 6H, CH_3-CH_2-); ^{13}C NMR (300 MHz, $CDCl_3$): δ = 178.92, 172.50 (C═O), 171.29, 162.80 (C═S), 139.33, 137.61 (C-Cl), 135.29, 131.01 (C_{para}–Ph), 130.44, 129.20 (C_{meta}–Ph), 129.15, 128.14 (C_{ortho}–Ph), 48.06,

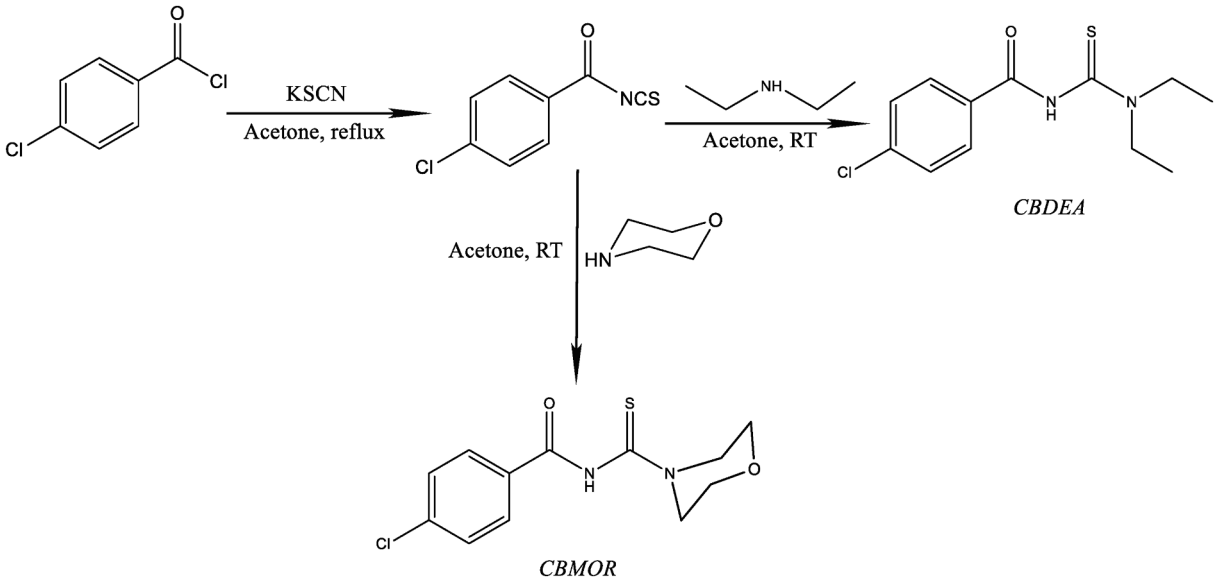

Scheme 1. Synthesis of *CBDEA* and *CBMOR*.

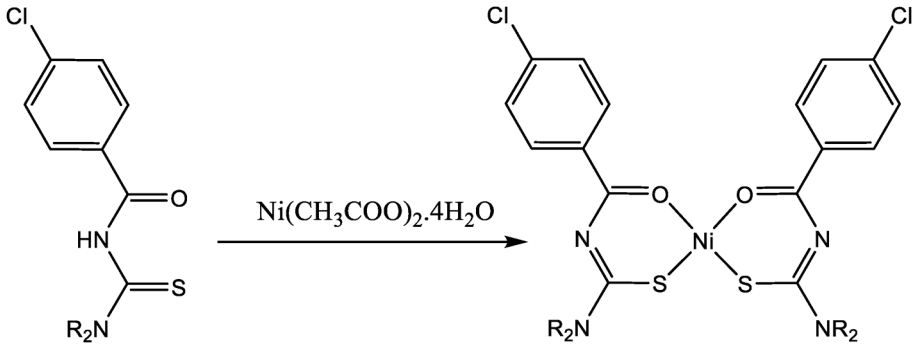

Scheme 2a. Synthesis of Ni(II) complexes of *CBDEA* (R = -CH_2CH_3) and *CBMOR* (R_2 = $O(CH_2CH_2)_2$).

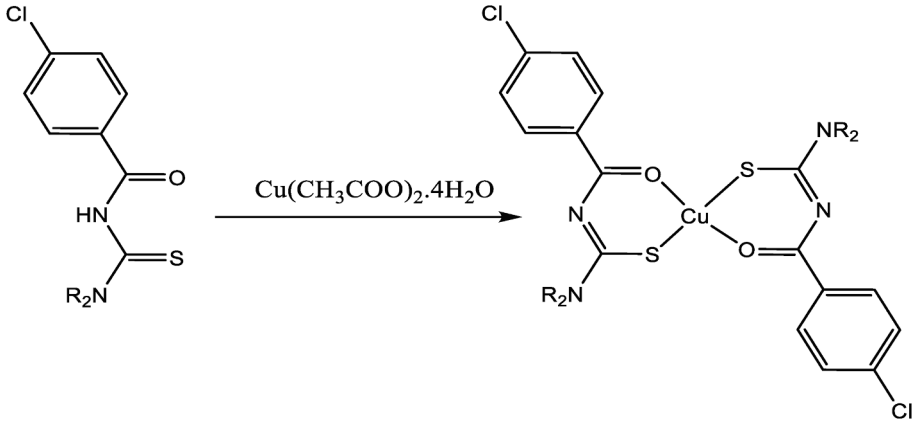

Scheme 2b. Synthesis of Cu(II) complexes of *CBDEA* (R = -CH_2CH_3) and *CBMOR* (R_2 = $O(CH_2CH_2)_2$).

47.74, 46.23, 45.60 (CH_2), 13.25, 13.12, 12.48, 11.49 (CH_3); IR (KBr) υ (cm^{-1}): 1590 (st, υC = O), 1251 (υC = S); UV: 274 nm (C═S, $n\rightarrow\pi^*$), 509 nm ($^1A_{1g}\rightarrow{}^1A_{2u}$).

2.3.2. bis(N,N-diethyl-N′-4-chlorobenzoylthioureato)copper(II) (CuCBDEA)

Colour: light green crystals; m.p: 176 °C, yield: 61 %, $C_{24}H_{28}Cl_2CuN_4O_2S_2$; Calculated %: C 47.80, H 4.68, N 9.29; Found %: C 47.92, H 4.62, N 9.31; IR (KBr) υ(cm^{-1}): 1575 (st, υC = O), 1250 (υC = S); UV: 274 nm (C═S, $n\rightarrow\pi^*$), 631 nm ($^2B_{1g}\rightarrow{}^2B_{2g}$).

2.3.3. bis(N-morpholine-N'-4-chlorobenzoylthioureato)nickel(II) (NiCBMOR)

Color: reddish brown; m.p: 270 °C (decomposed), yield: 74 %, $C_{24}H_{24}Cl_2N_4NiO_4S_2$; Calculated %: C 46.03, H 3.86, N 8.95; Found %: C 45.97, H 3.93, N 8.96; ^{1}H NMR (300 MHz, DMSO D_6): δ = 7.46 (d, 2H,

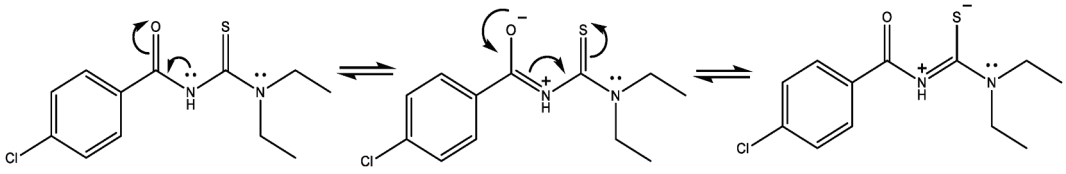

Scheme 3. Proposed delocalization pattern for N,*N*-diethyl-N'-(4-chlorobenzoyl)thiourea.

Ar-H), 7.40 (d, 2H, Ar-H), 4.36 (t, 2H, CH_2-CH_2), 3.29–3.69 (t, 6H, –CH_2-CH_2); ^{13}C NMR (100 MHz, DMSO D_6) δ: 174.50 (C═N), 171.20 (C═O), 162.80 (C═S), 139.33 (C-Cl), 133.26 (C_{para}–Ph), 128.14 (C_{meta}–Ph), 125.14 (C_{ortho}–Ph), 68.06 (-CH_2-CH_2- morpholine), 47.74 (-CH_2-CH_2- morpholine), IR (KBr): υ(cm^{-1}): 1591 (st, υC = O), 1290 (υC = S). UV: 276 nm (C═S, $n\rightarrow\pi^*$).

2.4. bis(N-morpholine-N'-4-chlorobenzoylthioureato)copper(II) (CuCBMOR)

Color: green; m.p: 256 – 258 °C, yield: 72 %, $C_{24}H_{24}Cl_2CuN_4O_4S_2$; Calculated %: C 45.68, H 3.83, N 8.88; Found %: C 45.66, H 3.87, N 8.85; IR (KBr): υ(cm^{-1}) 1593 (st, υC = O), 1270 (υC = S), UV: 274 nm (C═S, $n\rightarrow\pi^*$), 633 nm ($^2B_{1g}\rightarrow{}^2B_{2g}$).

2.5. X-ray crystallographic analysis

X-ray intensity data of *CBMOR* and *CBDEA* were measured at the University of Akron on a Bruker CCD-based diffractometer with dual Cu/Mo ImuSmicrofocus optics (Mo Kα radiation, λ = 0.71073 Å). Crystals were mounted on a cryoloop using Paratone oil and placed under a stream of nitrogen at 100 K (Oxford Cryosystems). The detector was placed at 5.00 cm from the crystal. The data were corrected for absorption with the SADABS program [24]. The structures were refined using the Bruker SHELXTL Software Package (Version 6.1). *NiCBDEA* and *CuCBDEA* diffraction data were collected at 105.9(4) K on an Oxford Rigaku four-circle diffractometer equipped with PhotonJet (Cu, λ = 1.54184 Å) X-ray source. Data integration, scaling, and empirical absorption correction were carried out using the CrysAlis-Pro program package [25]. The structures were solved with the intrinsic phasing method in ShelXT [26] and refined by Matrix-least-square against F^2 on ShelXL [27]. The non-hydrogen atoms were refined anisotropically, and hydrogen atoms were placed at idealized positions and refined using the riding model. The crystal structure of *CuCBDEA* had a disorder at the N(1)-C(1)-N(2) atoms and the adjourning ethyl groups; these were modeled in two positions with half occupancies on the atoms, with constraints on the bonds to stabilize the molecule. All calculations were implemented in OLEX2 program package [28]. X-ray diffraction data of *NiCBMOR* were recorded with a STOE IPDS II diffractometer at room temperature using graphite-monochromated Mo Kα radiation by applying the ω-scan method. Data collection and cell refinement were carried out using X-AREA [29], while data reduction was applied using X-RED32[29]. The structure was solved by direct methods with SIR2019 [30], and refined by means of the full-matrix least-squares calculations on F^2 using SHELXL-2018[27]. All H atoms were located in a difference electron-density map and then treated as riding atoms in geometrically idealized positions. Molecular graphics were created by using OLEX2 [28]. The crystallographic data and refinement parameters are summarized in Table 1.

2.6. DNA binding studies

2.6.1. UV titrations

The study compounds (about 1 mmol) were dissolved in DMSO (0.5 mL) and diluted in a 100 mM KCl, 10 mM Tris-HCl, and pH-7.5 buffer solution to the absorption titrations a final concentration of 20 μM [31]. Titrations were performed in a 10-mm stoppered quartz cell using a mixed concentration of each compound. The CT-DNA stock solution was added in increments of 2 μL, creating 4 μM additions, till no change in absorption spectrum was observed. Analyses were performed by means of a UV–Vis spectrophotometer by recording the spectrum after each addition of DNA. Ligand or complex-DNA solutions were mixed by using a Pasteur pipette and were incubated for 10 min each time before the spectra were recorded. Cell compartments were thermostated at 25 ± 0.1 °C. The stabilities of the compounds in titration conditions were tested by measuring the change in absorption for 4 h at 30 min intervals.

2.6.2. Gel Electrophoresis:

Gel electrophoresis experiments were performed according to the reported procedure [31], by using pBR322 negatively supercoiled plasmid DNA on 1 % agarose gels in 100 mM KCl, 10 mM Tris-HCl, and pH-7.5 buffer solution. Reaction mixtures (10 μL) containing 20 ng of pBR322 together with different concentrations of the study compounds (10, 25, 50, 100, 200 μM) were prepared in the same buffer at 0 °C, and then allowed to incubate at 25 °C for 1 h in the dark, and then in the presence of a peroxide solution. Before loading samples onto the gel, 2.5 mL of 0.25 % bromophenol blue loading buffer and sucrose in water (40 % w/v) were added to the reaction mixtures. Gels were obtained at room temperature by using a Thermo midi horizontal agarose gel electrophoresis system and applying a potential of 35 V for 4 h. The resulting gels were stained in ethidium bromide solution (0.5 mg mL^{-1}) for 45 min, after which they were further soaked in water for 20 min. Gels were visualized under U.V. light and photographed.

2.7. Antimicrobial assay

The biological activities of all the synthesized compounds against bacteria and fungi were determined by the disc diffusion method [32-35], and the minimum inhibitory concentrations (MIC) were obtained by the broth dilution method [36,37]. Seventeen bacteria and four fungi were tested. To test the antimicrobial activity of all the synthesized compounds, a Mueller Hinton Agar (MHA) plate was inoculated with a

Table 1
Some physical parameters of the compounds.

Compounds	Molecular formula	Color	% yield	Melting point (°C)	Molar conductivity ($ohm^{-1}mol^{-1}cm^{-2}$)
CBDEA	$C_{12}H_{15}ClN_2OS$	Colorless	89	156 – 158	–
NiCBDEA	$C_{24}H_{28}Cl_2N_4NiO_2S_2$	Red	75	222	1 ± 1
CuCBDEA	$C_{24}H_{28}Cl_2CuN_4O_2S_2$	Light green	61	176	3 ± 1
CBMOR	$C_{12}H_{13}ClN_2O_2S$	Colorless	90	146 – 148	–
NiCBMOR	$C_{24}H_{24}Cl_2N_4NiO_4S_2$	Reddish brown	74	270 (decomposed)	1 ± 1
CuCBMOR	$C_{24}H_{24}Cl_2CuN_4O_4S_2$	Green	72	256 – 258	2 ± 1

0.1 mL broth culture of bacteria or yeasts. Detailed procedure of the antimicrobial assay has been reported elsewhere [32].

2.8. Anti-proliferative studies

2.8.1. Cell culture

Two lines of human cancer cells were used in these experiments. Human prostate cancer PC-3 cells and human breast cancer MCF-7 cells were grown in RPMI-1640 and DMEM, respectively, and supplemented with 10 % FBS, 1 % L-glutamine, and 100 U/mL penicillin and streptomycin (Sigma). Cells were maintained in a humidified atmosphere with 5 % CO_2 air at 37 °C and incubated overnight. Cells in the exponential phase of growth were used in each experiment. The cells were seeded in 48 or 96 well plates with 10^5 cell densities. Apoptosis measurement was maintained in 24 wells and was carried out at a cell density of 10^6 cells per mL. After 24 h, different concentrations of study compounds (5, 10, 20, 40 μM) and 1 μM *paclitaxel* (*Pax*) were added to the well plates, and measurements were performed on the cells [38-40].

2.8.2. Cell survival assay

The toxicity of the compounds was evaluated by using 3-(4,5-dimethylthiazol-2-yl)-2,5-diphenyltetrazolium bromide tetrazolium (MTT) reduction assay on both cancer cells. For this, 5 mg/mL MTT dye was dissolved in PBS, and 40 μL was added to each well. After 4 h of incubation, formazan crystals were dissolved in DMSO and measured at 540 nm and 620 nm spectrophotometrically [38-40].

2.8.3. HOPI staining

Apoptosis was assessed by Hoechst and propidium iodide (HOPI) staining. The cells were seeded in a 24-well plate at a density of 10^6 cells/well. The day after, the cells were treated with the studied compounds. After treatments for 24 h, cells were washed with PBS, trypsinized, and centrifuged. Pellets were suspended in 50 μL fresh medium with addition of 0.25 μL of Hoechst and 0.25 μL of propidium iodide and incubated for 30 min at 37 °C in the dark. The cells were immediately analyzed by fluorescence microscopy, and images were taken by Zeiss axiocam ICc5 camera [38–40].

2.8.4. Statistical analyses

Statistical analysis was determined by using GraphPad Prism (GraphPad Software, Inc., La Jolla, CA, USA). Cytotoxicity values were expressed as mean ± SD of at least four independent experiments, the differences among the groups were analyzed by one-way analysis of variance (one-way ANOVA), and HOPI data were analyzed by two-way analysis of variance (two-way ANOVA). $p < 0.01$ and $p < 0.05$ were considered to be significant.

3. Results and discussion

3.1. Physical properties of the synthesized compounds

The acylthioureas and metal complexes were isolated by recrystallization using suitable solvents. The acylthioureas were soluble in warm organic solvents such as ethanol, methanol, and acetone, but highly soluble in dichloromethane, DMF, and DMSO. The metal complexes were colored non-hygroscopic and stable solids. They were slightly soluble in ethanol, methanol, and acetone. The nickel complexes are soluble in dichloromethane, DMSO, and DMF, while copper complexes are soluble in these solvents when hot. The low molar conductivity values of the metal complexes indicate that they are non-electrolytes [34,41,42]. Some physical parameters of the synthesized compounds are shown in Table 1.

3.2. Structural description of CBDEA, CBMOR, NiCBDEA, CuCBDEA, and NiCBMOR

The crystal structure refinement parameters of *CBMOR*, *NiCBMOR*, *CBDEA*, *NiCBDEA*, and *CuCBDEA* are presented in Table S1 of the supplementary information. Selected bond lengths and angles in the structures are shown in Tables S2 and S3. The molecular structure and atom numbering scheme of *CBDEA* is presented in Fig. 1. *CBDEA* crystallized in a monoclinic $P2_1/c$ space group with two molecules per unit cell. The molecule of *CBDEA* is non-planar with the *N*,*N*-diethyl moiety twisted out of the plane with the aromatic group. The conformation of the *CBDEA* molecule with respect to acylthiourea group was twisted as reflected by the C7-N1-C8-S1 and C1-C7-N1-C8 dihedral angles of 94.1° and −177.2°, respectively. These twist angles are quite low compared to the 3-chlorobenzoylthiourea derivatives previously reported [43]. The dihedral angle of *CBDEA* also reveals that the thiourea moiety is almost perpendicular to the chlorobenzoyl group. The twisting of conformation is a result of steric repulsion between the carbonyl C7-O1 group and the thiocarbonyl C8-S1 group, which was also confirmed by the S1-C8-N2 bond angle of 126.6(2)°. In *CBDEA*, the bond lengths of carbonyl (C7-O1) and thiocarbonyl (C8-S1) are 1.233(3) Å and 1.656(3) Å respectively, which are indicative of double bond character [22,43-45]. The C8-N2 and C7-N1 bond lengths of 1.327(3) and 1.355(3) Å respectively are shorter compared to the average C—N single bond length of 1.48 Å. This shows that the acylthiourea C—N single bonds possess partial double bond character, perhaps due to the conjugation of C═O and C═S π-electrons with lone pairs of electrons on nitrogen (Scheme 3) [44,46–48]. The elongation of the C8-N1 (1.431(3) Å) bond relative to C8-N2 (1.327(3) Å) and C7-N1 (1.355(3) Å) bonds agrees with literature reports [46,47]. Previous reports on chlorobenzoyl thiourea derivatives show that the longer the C═S bond, the shorter the C═O bond [43,44,49]. This serves as means to compensate for the repulsion between the two polar groups.

The molecular structure of *CBMOR* shown in Fig. 2 is similar to the structure of *CBDEA*. The conformation of the *CBMOR* molecule with respect to the thiourea moiety is non-planar, as reflected by the C5-N1-C6-N2 torsion angle of 62.0(2)°. The carbonyl oxygen is twisted away from the chlorophenyl plane, as seen from the C1-C4-C5-O2 torsion angle of −151.0°. The morpholine ring exhibits a chair conformation while the chlorophenyl ring is almost planar. The carbonyl C5-O2 (1.217 (2) Å) and thiocarbonyl C6-S1 (1.671(2) Å) bond lengths in *CBMOR* show a typical double bond character similar to the *CBDEA* structure [10,45,50]. The C—N bonds C5-N1 (1.392(2) Å), C6-N1 (1.409(2) Å), and C6-N2 (1.326(2) Å) are all shorter than the average single C—N bond lengths of 1.48 Å, thus showing varying degrees of partial double bond character [50–52]. The C6-N2 bond in the vicinity of the thiocarbonyl has a much shorter bond length than other C—N bonds in the molecule [47,50]. This shows the contribution of the thiol tautomeric form caused by the conjugation of the nitrogen lone pairs with the π electrons of the C═S. The bond lengths and angles in Table S2 are similar to those in chlorobenzoylthiourea derivatives reported in the literature [10,50,51]. Molecular aggregation in *CBDEA* (Fig. S1) and *CBMOR* (Fig. S2) show intermolecular hydrogen bonding between the thiourea N—H donor group and O acceptor of the morpholine [53].

The molecular structure of *NiCBDEA* is shown in Fig. 3, while selected bond lengths and angles are presented in Table S3. The *NiCBDEA* molecule crystallized with two independent molecules in the asymmetric unit. The crystal structure of *NiCBDEA* consists of a Ni(II) center coordinated to two anionic chlorobenzoyl thiourea moieties through S and O atoms in a distorted S_2O_2Ni square planar geometry [43,47]. The 6-membered metallacyclic ring formed on each side of the square plane consists of two carbon atoms, anionic S and O atoms, and deprotonated imine nitrogen. The S_2O_2Ni square plane is planar to a root mean square deviation of ~ 0.01 Å and ~ 0.023 Å in the two structures. The *cis* angles subtended at the Ni center for the two independent structures are slightly different. For example, the S1-Ni1-O1 angles in

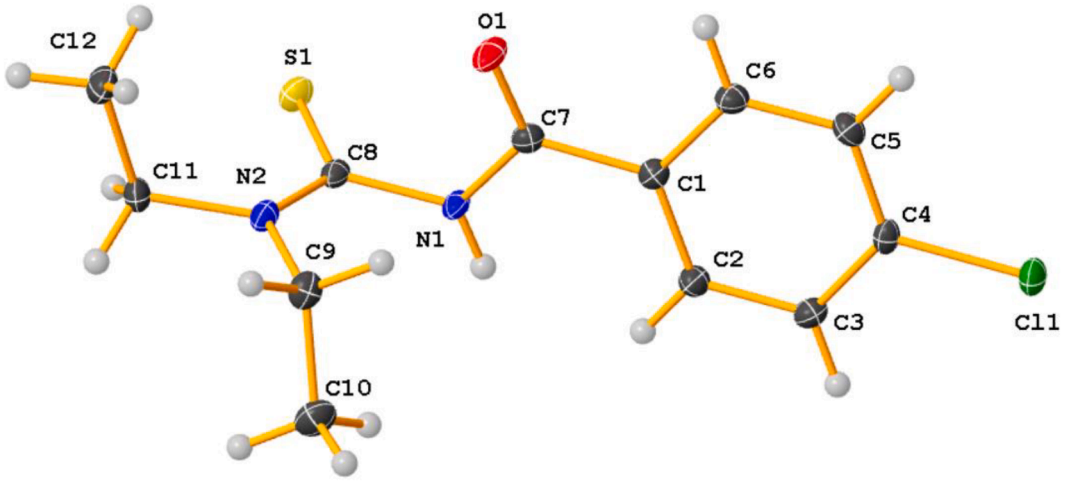

Fig. 1. Molecular structure of *CBDEA* showing the atomic numbering scheme at 30 % ellipsoids.

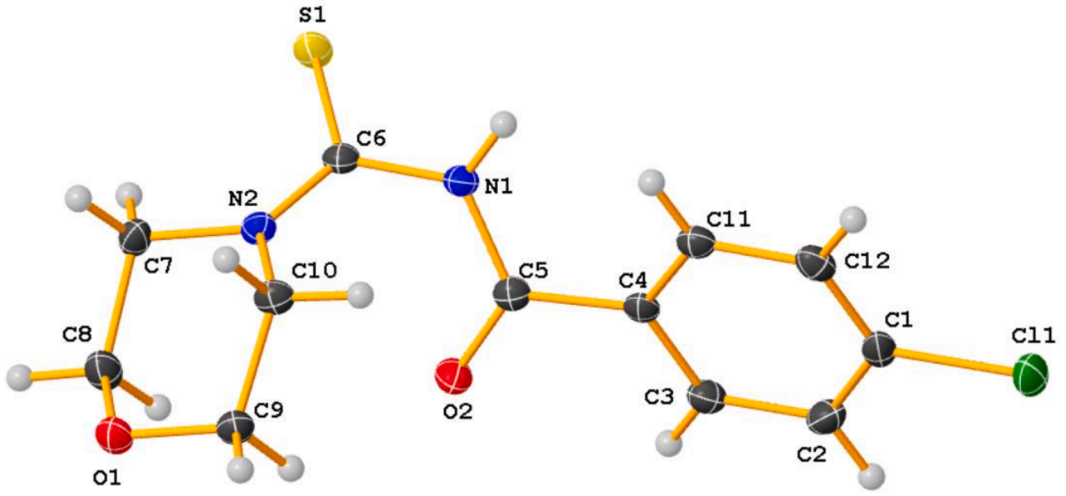

Fig. 2. Molecular Structure of *CBMOR*, showing the atomic numbering scheme at 30 % ellipsoids.

structures are 93.84(5)° and 94.46(5)°. A similar trend was observed with the O-Ni-S *trans* angles ranging from 176.53(5)° to 179.23(6)°. The magnitude of the *trans* angles in the structures is an indication that the coordination environment around the Ni atom is essentially planar. The C—N bonds in the structures are slightly shortened, while the C—S and C—O bonds are elongated when compared to the corresponding bonds in the structure of the thiourea ligand *CBDEA*. For instance, the C—N bond length was shortened from 1.431(3) Å in the ligand to 1.340(3) Å in the complex. The C—O and C—S bond lengths in *CBDEA* are 1.233(3) Å and 1.656(3) Å, respectively, while the corresponding bonds in *NiCBDEA* are 1.272(2) Å and 1.7316(19) Å, respectively. This is an indication of the delocalization of π electrons in the six-membered metallacyclic ring system on coordination [43,54,55].

The crystal structure of *CuCBDEA* is presented in Fig. 4. The compound crystallized in the monoclinic crystal system $P2_1/n$ space group with one-half of the molecule in the asymmetric unit. The symmetry elements in the molecule include an inversion center on the Cu metal center. The crystal structure has a disorder at the metallacyclic N1A-CIA bond, including the adjacent diethylamine moiety, and this was modeled in two positions with half occupancies for the atoms involved. A few RIGU constraints were put in place to stabilize the refinement. Information relating to the geometric parameters, coordination, geometry, and the symmetry of the metal complex was successfully obtained from one half of the compound. The coordination geometry of the *CuCBDEA* is similar to that in *NiCBDEA* discussed earlier, with two *CBDEA* molecules coordinated to Cu(II) through O and S atoms in a slightly distorted square-planar geometry. However, unlike in *NiCBDEA*, the O and S coordinated to the Cu(II) ion in *CuCBDEA* in a *trans* fashion, a unique geometry in acylthiourea based metal complexes as they often adopt the *cis* conformations [43,56,57]. In any case, the synthesis of *cis* and trans diethylamine acylthiourea derivatives using different Cu salts has been reported [43,56-58]. The mechanism of *cis–trans* isomerization observed in this group of compounds is not clearly extablished yet, however a number of factors including electronic properties of the ligand and solvent polarity have been fingered as the driving forces for *cis–trans* isomerization in alkyl-substuted thiourea complexes [59,60]. The O-Cu-S *cis* angles of 86.30(9)° and 93.70(9)° are indicative of the square planar configuration of the complex. The S1-Cu1-S1 and O1-Cu1-O1 bond angles of approximately 180° show the symmetrical nature of the structure with an inversion center at the Cu atom. The difference in the Cu–O and Cu-S bond lengths of 1.912(3) Å and 2.2529(10) Å in the present complex is due to the difference in *trans* influence of the O and S donor atoms on the metal *d*-orbital. These M−S/O bond lengths in CuCBDEA are conspicuously longer than the corresponding bonds in NiCBDEA probably due the occupation of the $d(x^2\text{-}y^2)$ orbital in the Cu and subsequent Jahn teller distortion. Similar trends have been reported for related acylthiourea copper(II) complexes [43,56,58].

The molecular structure of *NiCBMOR* is in Fig. 5, is similar to

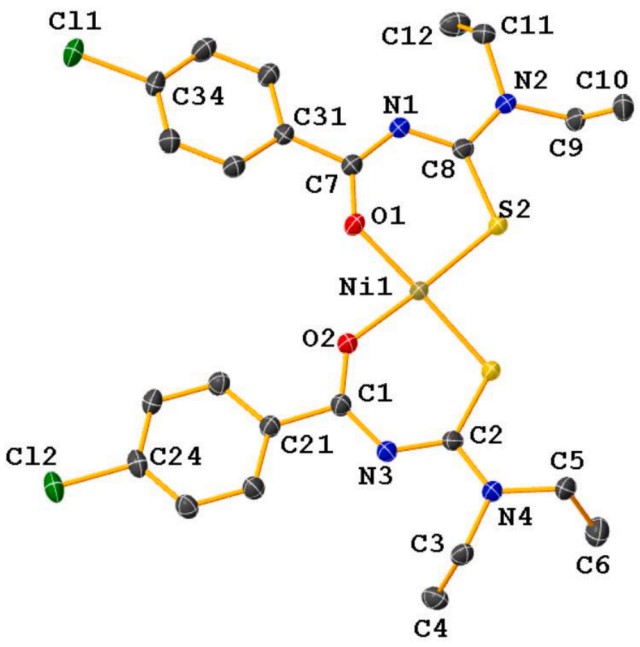

Fig. 3. Molecular structure of *NiCBDEA* showing the atomic numbering scheme at 30 % ellipsoids. Some phenyl ring atom numbering and one of the two independent structures are omitted for clarity.

NiCBDEA where *CBMOR* ligands are coordinated to the central Ni(II) ion in a monometallic biconnected pattern through two chalcogen atoms, resulting in a bicyclic system with a *cis*-square-planar NiO_2S_2 core. The angle between the planes formed by Ni1/O1/S1 and Ni1/O3/S2 atoms is 11.37(9)°. In the square-planar coordination, the intraligand S—Ni—O angles averaging 94.69(6)° are considerably larger than the interligand S—Ni—S and O—Ni—O angles of 86.17(3)° and 86.64(8)°, respectively. The *cis* angles varying from 86.17(3)° to 94.75(6)° and the *trans* angles ranging from 171.09(8)° to 172.27(7)° deviate significantly from their ideal values of 90° and 180°. These are similar to values found in *NiCBDEA*. There is no significant difference between the Ni1—S1 and Ni1—S2 bond distances of 2.1430(7) and 2.1516(8) Å, respectively. The Ni1—O1 and Ni1—O3 bond distances of 1.8739(19) and 1.8755(17) Å, respectively, are equal within the experimental errors. Both Ni—S and Ni—O lengths are comparable with those in *NiCBDEA* and other square-planar NiO_2S_2 complexes in the literature [61-67]. The C8—S1 and C20—S2 bond distances of 1.739(3) and 1.738(3) Å, respectively, are consistent with the single bond character, demonstrating that the ligands are bound to nickel in thiolate form. The ligand is monoanionic and coordinates in its keto form, which can be verified from the C7—O1 and C19—O3 bond lengths of 1.278(3) and 1.275(3) Å, respectively. The chelate ring bond distances demonstrate the delocalization of π-electrons. The packing structure of NiCBMOR is shown in Fig. S4.

3.3. Spectroscopic studies

The characteristic I.R. bands, ^{1}H NMR and U.V.-vis are presented in the experimental section, and they confirm the structures of the compounds. In the I.R. spectra of the ligands, the characteristic N—H stretching vibration peak was observed at 3271 cm^{-1} (*CBDEA)*, 3258 cm^{-1}(*CBMOR)* [44]. The N—H stretching peak disappeared upon complexation. This deprotonation led to the delocalization of the π electrons on the OC-*N*-CS system. This is consistent with literature reports [16,44] and supports the formation of the metal complexes.

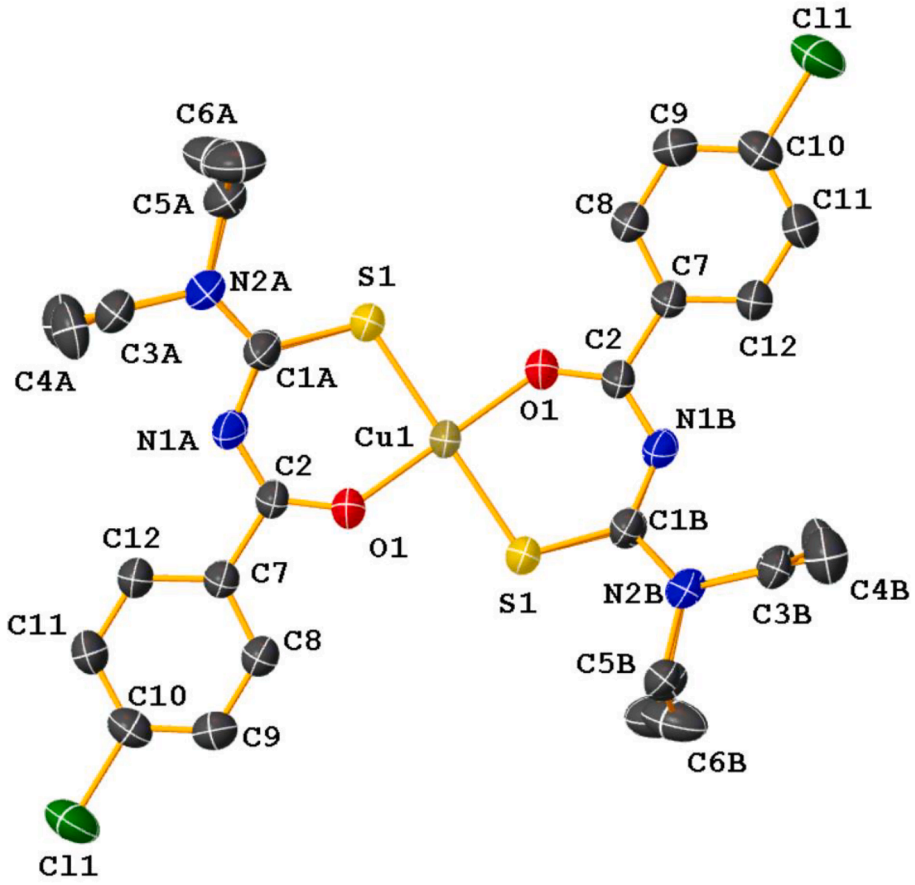

Fig. 4. Molecular structure of *CuCBDEA* showing the atomic numbering scheme at 30 % ellipsoids.

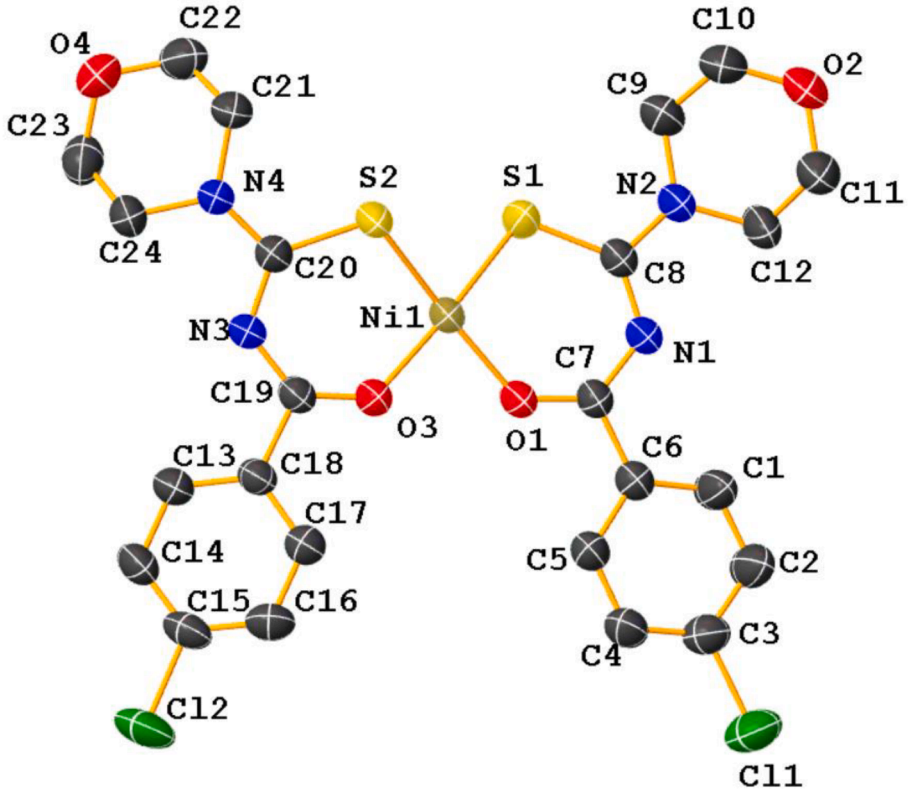

Fig. 5. Molecular structure of *NiCBMOR* showing the atom numbering scheme. Displacement ellipsoids are drawn at the 30 % probability level.

CBDEA and *CBMOR* showed single peaks at 1642 cm^{-1} and 1686 cm^{-1}, respectively which were due to C═O stretching vibration [44,45,53]. These peaks were observed at lower frequencies in the metal complexes (*CuCBDEA*, 1575 cm^{-1}; *NiCBDEA*, 1590 cm^{-1}; *CuCBMOR*, 1593 cm^{-1}; *NiCBMOR*, 1591 cm^{-1}), suggesting coordination through the oxygen atom [14,44]. The ^{1}H NMR spectra of CBDEA and CBMOR are consistent with structural information provided by the single-crystal X-ray diffraction studies. The characteristic N—H proton signal appeared at 10.62 ppm (*CBDEA*) and 10.82 ppm (*CBMOR*). The aromatic protons of *CBDEA* were observed in the range of 7.54–7.90 ppm while that of *CBMOR* were observed from 7.56 – 7.93 ppm. The aliphatic proton signals and *CBDEA* were found in the upfield region of the spectra in the range of 1.14–3.93 ppm. The triplet peaks at 1.20 and 1.14 ppm were assigned to $–CH_3$ protons, while the quartet peaks between 2.44 and 3.93 ppm were assigned to $–CH_2$-N of the diethyl group. In the ^{1}H NMR spectra of *CBMOR,* the morpholine ring protons were observed as triplets at 3.71–3.57 ppm. The ^{13}C NMR spectra of *CBDEA* and *CBMOR* are also consistent with structural information provided by the single-crystal X-ray diffraction studies. The C═O groups were observed around 179–178 ppm, and the peaks for C═S and C-Cl are seen around 162–139 ppm. The values of elemental analysis of compounds shown in the experimental section, are in agreement with their molecular formula. The U.V./vis spectra of *CBDEA, CBMOR* and metal complexes were recorded in ethanol/DMSO. The absorption band were observed in the range at 274–281 nm were due to the π*←n electronic transition of the C═S bond [22]. Bands assignable to d←d transitions were also observed at 509 nm for *NiCBDEA* and 633 nm for *CuCBMOR*.

3.4. DNA binding studies

3.4.1. UV titrations of the ligand and the complexes

The DNA interactions were initially monitored by U.V. spectrophotometry by using the most common and valid methods [68]. The addition of DNA to the solutions of the compounds caused changes in the U. V. absorbances, which is an indication of DNA interactions. First, the stability of the compounds in aqueous was studied by using U.V. analysis against the time frame before the DNA titrations. All compounds, except *NiCBMOR* were stable at the interaction conditions for at least 4 h, giving no change in absorption spectra. The DNA titrations were monitored by using U.V. spectrophotometry and the results of the ligands and the complexes are shown in Fig. 6. *CBDEA* and *CBMOR* had U. V. absorptions at 274 nm and 279 nm, respectively. When DNA was incrementally added to the ligands the absorption increased, indicating external interaction with DNA. The acylthiourea functions of ligands may be protonated under the titration conditions and interact with negatively charged phosphate groups of DNA. On the other hand, *CuCBDEA*, *CuCBMOR*, and *NiCBDEA* complexes have an additional LMCT absorption band around 330 nm which instantly decreased (hypochromic effect) on interaction with the DNA. This is suggestive of stronger interaction between the metal complexes and DNA. The hypochromic effect without shift at the wavelength generally indicates a DNA groove binding type of interaction of the compounds [68].

To quantitatively compare the DNA-binding affinities of the ligand and the complexes, the intrinsic binding constants K_b of the complexes to DNA were obtained by monitoring the changes of the π*←n and LMCT absorbance at around 300 nm for ligands and metal complexes, respectively according to the equation below.

$$\frac{[DNA]}{\varepsilon_A - \varepsilon_f} = \frac{[DNA]}{\varepsilon_B - \varepsilon_f} + \frac{1}{K_b(\varepsilon_B - \varepsilon_f)}$$

where [DNA] is the concentration of the nucleic acid in base pairs, ε_A is the apparent absorption coefficient obtained by calculating A_{obs}/[Drug], and $\varepsilon_f$and ε_b are the absorption coefficients for the free and the fully bound compounds, respectively. In the [DNA]/($\varepsilon_A - \varepsilon_f$) versus [DNA] plot, K_b is given by the ratio of the slope to the intercept [68]. The ligands have very low affinity while the complexes have moderate affinities to DNA (Table 2) comparable to other complexes in the literature [69-71].

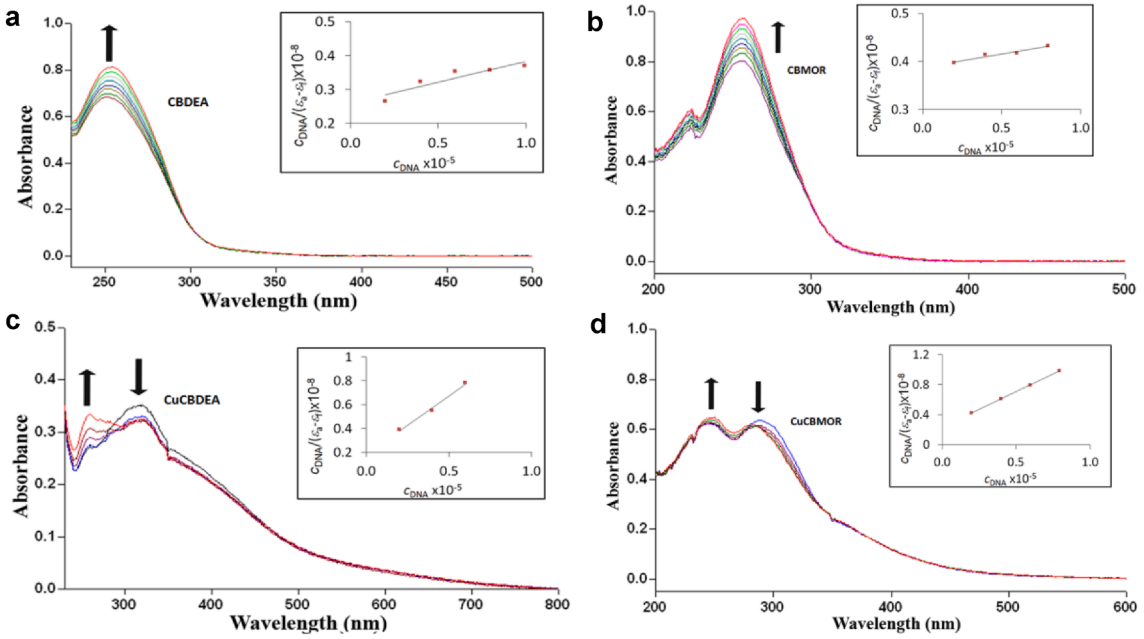

Fig. 6. Absorption spectra of the ligands and complexes in 5-mM Tris-HCl buffer (pH 7.5) upon the addition of CT-DNA. (a) *CBDEA*, (b) *CBMOR*, (c) *CuCBDEA*, and (d) *CuCBMOR*. *NiCBDEA* is presented in Fig. S17 of the Supporting Information. The concentration of the ligand and complexes = 20 μM; [DNA] = 0–5 μM. Arrow shows the absorbance changing upon the increase of DNA concentration.

Table 2
Binding constants for the ligand and the metal complexes.

Compounds	Binding constants (K_b) 10^{-5} M^{-1}
CBDEA	0.031
CuCBDEA	0.55
NiCBDEA	4.4
CBMOR	0.015
CuCBMOR	4.04

3.4.2. Cleavage of pBR322 DNA by the metal complexes

The potential of the complexes to cleave DNA was studied by gel electrophoresis using supercoiled pBR322 DNA in 100 mM KCl, 10 mM Tris-HCl, pH-7.5 buffer. The plasmid DNA is naturally in intact supercoil form (I) and a relatively fast migration will be observed when subjected to gel electrophoresis. Small damage causes the supercoil to relax, generating an open circular form (II) which moves slower in the gel. More damage creates a linear form (III) that migrates between (I and II) [68]. Severe damage causes digestion of DNA creating small pieces which are not visible in the gel [72-76]. Fig. S17 shows gel electrophoresis separation of pBR322 after incubation with each of the ligands and complexes with increasing concentrations (A) and also with the addition of peroxide solution (B). *CBDEA* and *CBMOR* had no effect on DNA under both conditions. The complexes alone (A) also did not cause any damage in the plasmid DNA. However, copper complexes *CuCBDEA* and *CuCBMOR* severely damaged DNA in the presence of peroxide, creating very small DNA pieces which are not visible in the gel at high concentrations (lanes 6 and 7; 100 and 200 μM). This is due to Cu(II) to Cu(I) redox reaction, which generates radical ions from peroxide that hydrolyze DNA phosphate linkages [7,77-79] *CuCBMOR* also shows form III of DNA, indicating a higher degree of DNA damage at the 50 μM concentration (lane 5) before it disappears at the higher concentrations (lanes 6–7).

NiCBDEA results in a different pattern of damage on DNA structure in the presence of peroxide. A high amount of Form II and Form III formations resulting from the addition of *NiCBDEA* at 50–200 μM concentrations (lanes 5–7) indicates DNA damage. All the metal complexes induce DNA damage which would create some degree of inhibition of the DNA function such as transcription and/or replication. This will in-turn induce cell death [7,77,79]. However, the nature of reactive intermediates involved in the DNA-cleavage by the complexes is not clear yet. Further studies on the mechanism are currently underway.

3.5. In vitro antimicrobial assay

The results of antimicrobial activities of the study compounds and the reference antibiotics reported as inhibition zone diameter (mm) are shown in Table S4 of the Supporting Information. The minimum inhibitory concentration (MIC) values which suggested that some of the studied compounds exhibited considerable antimicrobial activity are shown in Table S5. Fig. 7 shows a comparison of the minimum inhibitory concentrations (MIC, μgmL^{-1}) of *CBDEA*, *CBMOR*, and the control drugs, *streptomycin* and *fluconazole*.

In general, *CBDEA* exhibited better antimicrobial properties compared to *CBMOR*; while *CBDEA* was active against 67 % of all the microbial strains studied, *CBMOR* was active against about 43 %, and the antimicrobial activity was somewhat diminished on complexation. The superior antimicrobial activity of *CBDEA* is further reflected in the fact that it exhibited better activity against Gram-negative bacterial strains *P. Aeruginosa* ATCC 35032, *K. pneumoniae* ATCC 13882 and *S. marcescens* ATCC 13880. Generally, all the studied compounds showed relatively higher antimicrobial activity against the Gram-positive bacteria and the fungi strains, which is consistent with previous report [9,46]. The cell walls of Gram-negative bacteria are noted for having two membranes, made up of outer lipopolysaccharide (LPS) molecules and inner anionic phospholipids, while Gram-positive bacteria possess only one membrane made up of phospholipids [7,74,75,77,79]. A good antimicrobial agent is expected to cause cell leakage by disrupting the membranes or cross the membranes barriers into the cell to obstruct cellular processes and thereby destroy the bacteria [77]. It is therefore envisaged that Gram-negative bacteria membranes will be less accessible to membrane-targeting antimicrobials.

Lipophilicity has been reported as an important factor for the antimicrobial action of drugs [80,81]. The calculated logP (a measure of lipophilicity) of *CBDEA* (2.85 ± 0.60) compared to *CBMOR* (1.01 ± 0.64) is an indication that *CBDEA* has a better lipophilic character

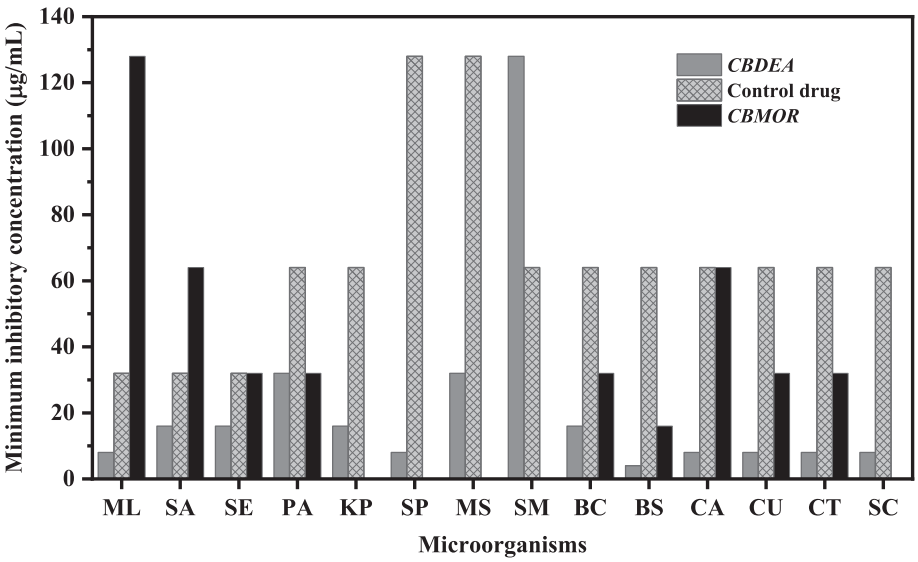

Fig. 7. Comparing the minimum inhibitory concentration (MIC, µg/mL) of *CBDEA*, *CBMOR* and control drug (streptomycin for antimicrobial and fluconazole for antifungal). A lower value of MIC indicates higher activity. ML = *Micrococcusluteus* ATCC 9341, SA = *Stapylococcus aureus* ATCC 25923, SE = *Stapylococcus epidermidis* ATCC 12228, PA = *Pseudomonas aeruginosa* ATCC 35032, KP = *Klebsiella pneumoniae* ATCC 13882, SP = *Streptococcus pneumoniae* ATCC 27336, MS = *Mycobacterium smegmatis* ATCC 607, SM = *Serratia marcescens* ATCC 13880, BC = *Bacilllus cereus* ATCC 11778, BS = *Bacillus subtilis* ATCC 6633, CA = *Candida albicans* ATCC 10231, CU = *Candida utilis* ATCC 9950, CT = *Candida trophicalis*, SC = *Saccharomyces cerevisiae* ATCC 976.

[80,82]. The conformational rigidity of *CBDEA* and its more effective interactions with LPS of *P. aeruginosa* ATCC 35032, *K. pneumoniae* ATCC 13882 and *S. marcescens* ATCC 13880 may be essential for its more potent antimicrobial action against these strains [79]. *CBDEA* demonstrated antimicrobial activity against the Gram-positive bacterial strains in increasing order as follows; *S. aureus* ATCC 25923, *B. cereus* ATCC 11778, *S. epidermidis* ATCC 12228, *M. luteus* ATCC 9341 and *B. subtilis* ATCC 6633. *CBDEA* was also active against all the fungi. On the other hand, *CBMOR* exhibited (though relatively lower) antimicrobial activity against the microbes in increasing order as follows; *M. luteus* ATCC 9341, *S. aureus* ATCC 25923, *S. epidermidis* ATCC 12228, *B. cereus* ATCC 11778, *P. aeruginosa* ATCC 35032 and *B. subtilis* ATCC 6633. *CBMOR* showed antimicrobial activity against 3 of the 4 fungi strains studied. The Ni complexes of both ligands had better antimicrobial property compared to the Cu complexes. *NiCBDEA* was active against 13 microbes while *CuCBDEA* was active against only 4 microbes.

MICs were determined for the compounds that showed appreciable growth inhibition zones; the study was restricted to microorganisms that were affected by the compounds. From the results, MIC of selected compounds against bacterial and yeast pathogens varied from 4 to 256 $\mu g mL^{-1}$. The lowest MICs were observed for *CBDEA* (4–16 $\mu g\ mL^{-1}$) against *M. luteus,* ATCC 9341, *S. aureus* ATCC 25923, *S. epidermidis* ATCC 12228, *K. pneumoniae* ATCC 13882, *S. pneumoniae* ATCC 27336, *B. Cereus* ATCC 11778, *B. subtilis* ATCC 6633, *C. albicans* ATCC 10231, *C. utilis* ATCC 9950, *C. tropicalis* and *S. cerevisiae* ATCC 9763. The results suggest that *CBDEA* and the Ni(II) complexes of both ligands show promising antimicrobial activities against the studied bacteria and yeasts and are most likely good candidates for further investigation as antimicrobial agents.

3.6. Anti-proliferative studies

The results of the anti-proliferative activities of the study compounds and control drug MCF-7 cells are presented in Table 3, Figs. 8 – 9. The results on PC-3 cells are shown in Figs. S18 – S19 of the Supporting Information. Table 3 shows the values of IC_{50} on apoptotic cells and necrotic cells. In the figures, the cytotoxic effects of drugs against cancer cells and the ratios of the cell death types are presented. All the compounds show moderate to high activities against the tested cell lines. *CBMOR* showed much higher potency on MCF-7 cells compared to *CBDEA,* while their activity values on PC-3 cells are similar. The anti-proliferative activities were enhanced in the Cu(II) complexes, while the activities of the Ni(II) complexes is comparable to those of the free ligands or decreased. Anticancer activity of breast (MCF-7) and prostate (PC-3) cancer cells of *CuCBMOR* and *CuCBDEA* are more pronounced than *NiCBDEA*. Ni(II) complexes display *cis* conformation, while Cu(II) complexes exhibit *trans* conformation confirmed by crystal structure determination in this study. It is, therefore, apparent that the *CuCBMOR* and *CuCBDEA* exhibited better anticancer activity than *NiCBDEA*.

Table 3
The IC_{50} values and apoptotic cell rate of the compounds against the study cell lines.

Compounds	Cell line/IC_{50} (µM)		Cell line apoptotic rate	
	MCF-7	PC-3	MCF-7	PC-3
CBDEA	10 ± 2	15 ± 5	88 ± 5	87 ± 4
CuCBDEA	9 ± 10	11 ± 5	86 ± 4	91 ± 2
NiCBDEA	11 ± 6	20 ± 6	85 ± 4	83 ± 4
CBMOR	4 ± 6	18 ± 6	88 ± 2	77 ± 4
CuCBMOR	2 ± 1	2 ± 2	92 ± 1	86 ± 2
Control	–	–	6 ± 2	4 ± 2

CBMOR and *CuCBMOR* were very effective against the MCF-7 cell lines with IC_{50} values of 4.1 µM and 1.76 µM, respectively, and *CuCBMOR* showed high activity against the PC-3 cell lines. Judging from the IC_{50}, the potency of *CuCBMOR* is comparable to that of the control drug, *paclitaxel*. This is a strong effect for a novel compound, and this high activity for *CBMOR* and *CuCBMOR* against MCF-7 and PC-3 cells will increase interest in the development of morpholine-based anticancer agents. The higher activity of *CBMOR* and *CuCBMOR* can be linked to the morpholine moiety. Compounds with morpholine moieties have been well studied as anticancer agents, and commercially available anticancer drugs aprepitant and gefitinib contain morpholine fragments in their structure [83,84]. The cytotoxicity of *CuCBMOR* was ~ 2 fold and ~ 10 fold higher compared to *CBMOR* against MCF-7 and PC-3 cell lines, respectively.

Copper is a well-known bio-essential metal ion; its redox switching and tunable coordination geometry ensure DNA-binding and bioactivity [85-87]. The development of anticancer agents with endogenous metals such as copper is important as they are less toxic to normal cells compared to cancer cells. However, copper can also be toxic due to its affinity for redox reactions and the ability to substitute other essential metals in the active site of proteins and DNA [67]. Also, Cu(II) ion can bind to both hard and soft bases, thus enacting its effect, which can be positive or negative. To further investigate the cytotoxicity of the studied compounds, the apoptotic rates on MCF-7 and PC-3 cell lines

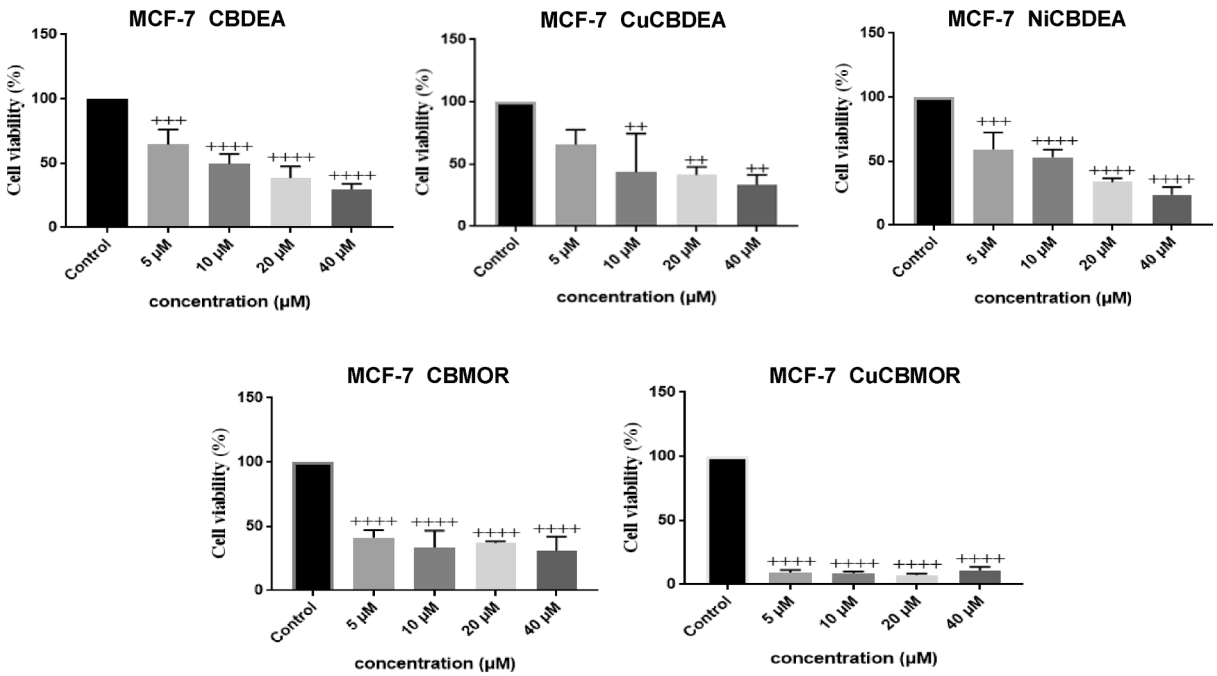

Fig. 8. The cytotoxicity of study compounds with untreated control groups on MCF-7 cells. The data were represented as mean ± standard error of the mean. A comparison was performed by the One Way ANOVA test with Dunnett's multiple comparison test applied as a post-hoc test. *p*-values equal or<0.05 were considered as statistically significant ($+p < 0.05$, $++p < 0.01$, $+++p < 0.001$, $++++p < 0.0001$) versus untreated control.

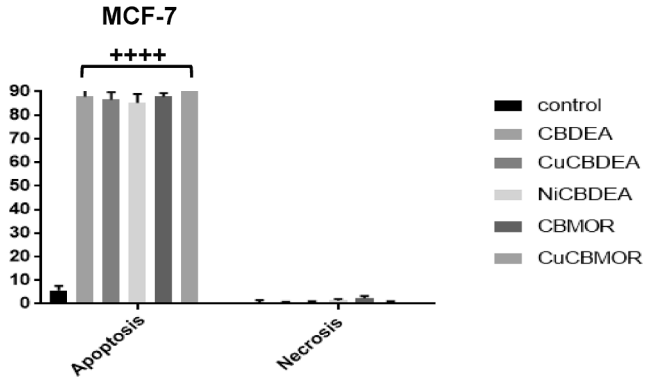

Fig. 9. Apoptosis measurement of study compounds on MCF-7 cells. The data were represented as mean ± standard error of mean. Comparison was performed by One Way ANOVA test with Dunnett's multiple comparison test was applied as a post-hoc test. *p*-values equal or<0.05 were considered as statistically significant ($+p < 0.05$, $++p < 0.01$, $+++p < 0.001$, $++++ p < 0.0001$) versus untreated control.

were investigated. From the apoptotic studies, a large amount of the cells died after the application of the compounds via apoptotic mechanisms. (Fig. 9). In Table 3, the apoptosis rate of the compounds and the control drug is given. The apoptosis ratios observed for the most effective derivative *CuCBMOR* was 91.53 % for MCF-7 cells and 85.95 % for PC-3 cells.

4. Conclusion

Two acylthiourea derivatives *N*,*N*-diethyl-*N*′-(4-chlorobenzoyl)thiourea (*CBDEA*), *N*-morpholine-*N*′-(4-chlorobenzoyl)thiourea (*CBMOR*) and their Ni(II) and Cu(II) complexes were synthesized. The ligands behaved as monoanionic bidentate molecules, coordinating through the thiol sulfur and the carbonyl oxygen. Four coordinate square-planar geometries were observed for the Ni(II) and Cu(II) complexes with *NiCBDEA* in *cis* geometry and *CuCBDEA* in *trans*, a similar coordination geometry observed in Pt(II) anticancer compounds. *In-vitro* screening of the compounds against some Gram-positive bacteria, Gram-negative bacteria, and yeasts confirmed the superior antimicrobial potencies of the *CBDEA* and its Ni(II) complex as compared to other studied compounds. Additionally, metal complexation did not lead to improved antimicrobial properties. *CBDEA* and *CBMOR* did not affect DNA under the experimental conditions; however, the copper complexes, *CuCBDEA* and *CuCBMOR*, severely damaged DNA in the presence of peroxide. The results of anti-proliferation tests indicated that *CuCBMOR* has the most effective anticancer activity with IC_{50} values of 1.76 μM for MCF-7 and 1.97 μM for PC-3, which is comparable to values obtained for *paclitaxel*, a well-known cancer drug. The apoptosis ratios observed for *CuCBMOR* (91.53 % in MCF-7 cell line and 85.95 % in PC-3 cell line) is a strong indication that it is a potential anticancer agent.

Declaration of Competing Interest

The authors declare that they have no known competing financial interests or personal relationships that could have appeared to influence the work reported in this paper.

Acknowledgement

The authors are grateful to the Department of Chemistry, Akron University, for assistance with X-ray crystal structure determination of *CBDEA* and *CBMOR*, School of Chemical Sciences, University of Auckland, New Zealand for crystal data of *NiCBDEA* and *CuCBDEA* and Scientific Research Projects Unit of Ondokuz Mayıs University (Project No: PYO.FEN.1906.19.001), Turkey for *NiCBMOR*. Many thanks to National Centre for Energy Research and Development, University of Nigeria, Nsukka for infrastructural support.

Appendix A. Supplementary data

CCDC 2009344, 2065533, 2009343, 2012502 and 2012503 contain the supplementary crystallographic data for *CBMOR*, *NiCBMOR, CBDEA*,

NiCBDEA and *CuCBDEA*, respectively. These data can be obtained free of charge on application to CCDC, 12 Union Road, Cambridge CB2 1EZ, UK [Fax: +44 1223 336 033, e-mail: deposit@ccdc.cam.ac.uk, https://www.ccdc.cam.ac.uk/structures/]. Supplementary data to this article can be found online at https://doi.org/10.1016/j.ica.2021.120590.

References

[1] G. López-Abente, S. Mispireta, M. Pollán, Breast and prostate cancer: an analysis of common epidemiological features in mortality trends in Spain, BMC Cancer 14 (1) (2014) 874.
[2] C.H. Marshall, et al., Prevalence of DNA repair gene mutations in localized prostate cancer according to clinical and pathologic features: association of Gleason score and tumor stage, Prostate Cancer 22 (1) (2019) 59–65.
[3] N.P. Barry, P.J. Sadler, Exploration of the medical periodic table: towards new targets, Chem. Commun. 49 (45) (2013) 5106–5131.
[4] J.D. Hoeschele, In remembrance of Barnett Rosenberg, Dalton Trans. 48 (2009) 10648.
[5] C. Hemmert, et al., Preparation, characterization and crystal structures of manganese (II), iron (III) and copper (II) complexes of the bis [di-1, 1-(2-pyridyl) ethyl] amine (BDPEA) ligand; evaluation of their DNA cleavage activities, J. Biol. Inorg. Chem. 6 (1) (2001) 14–22.
[6] M. Mrksich, P.B. Dervan, Antiparallel side-by-side heterodimer for sequence-specific recognition in the minor groove of DNA by a distamycin/1-methylimidazole-2-carboxamide-netropsin pair, J. Am. Chem. Soc. 115 (7) (1993) 2572–2576.
[7] S. Kumar, A. Pandey, Chemistry and Biological Activities of Flavonoids: An Overview, Sci World J. (2013).
[8] C. Sacht, et al., J. Chem. Soc., Dalton Trans. (2000).
[9] R. del Campo, et al., N-benzoyl-N′-alkylthioureas and their complexes with Ni (II), Co (III) and Pt (II)–crystal structure of 3-benzoyl-1-butyl-1-methyl-thiourea: activity against fungi and yeast, J. Inorg. Biochem. 98 (8) (2004) 1307–1314.
[10] A. Saeed, M. Parvez, The crystal structure of 1-(4-chlorophenyl)-3-(4-methylbenzoyl) thiourea, Open Chem. 3 (4) (2005) 780–791.
[11] S. Mohammad Shoaib et al., Acute toxicity, brine shrimp cytotoxic, antioxidant and analgesic activities of synthesized 1-benzoyl-3-methyl thiourea, 2014.
[12] M. Gemili, et al., Pt (II) and Ni (II) complexes of octahydropyrrolo [3, 4-c] pyrrole N-benzoylthiourea derivatives: Synthesis, characterization, physical parameters and biological activity, Inorg. Chim. Acta 463 (2017) 88–96.
[13] V. Ravichandran, et al., Prediction of anti-hiv activity of phenyl ethyl thiourea (pet) derivatives: qsar approach, Digest J. Nanomater. Biostruct. 4 (1) (2009).
[14] H. Arslan, N. Külcü, U. Flörke, Synthesis and characterization of copper (II), nickel (II) and cobalt (II) complexes with novel thiourea derivatives, Transition Met. Chem. 28 (7) (2003) 816–819.
[15] A.J. Hoey, et al., Characteristics of cyanopindolol analogues active at the β3-adrenoceptor in rat ileum, Br. J. Pharmacol. 119 (3) (1996) 564–568.
[16] M. Al-Ghorbani, et al., Piperazine and morpholine: Synthetic preview and pharmaceutical applications, Res. J. Pharm. Technol. 8 (5) (2015) 611–628.
[17] V. Kumar, S. Chimni, Anticancer Agents Med, J. Chem. 15 (2015) 163.
[18] D.P. Gouvea, et al., 2-Aryl-3-(2-morpholinoethyl) thiazolidin-4-ones: synthesis, anti-inflammatory in vivo, cytotoxicity in vitro and molecular docking studies, Eur. J. Med. Chem. 118 (2016) 259–265.
[19] F. Arshad, et al., Revealing quinquennial anticancer journey of morpholine: A SAR based review, Eur. J. Med. Chem. 167 (2019) 324–356.
[20] U. Solmaz, et al., Synthesis, characterization, crystal structure, and antimicrobial studies of novel thiourea derivative ligands and their platinum complexes, J. Coord. Chem. 71 (2) (2018) 200–218.
[21] J.K. Barton, A.L. Raphael, Photoactivated stereospecific cleavage of double-helical DNA by cobalt (III) complexes, J. Am. Chem. Soc. 106 (8) (1984) 2466–2468.
[22] J.N. Asegbeloyin, et al., Synthesis, structure, computational and in-silico anticancer studies of N, N-diethyl-N′-palmitoylthiourea, J. Mol. Struct. 1153 (2018) 69–77.
[23] I.B. Douglass, F. Dains, Some Derivatives of Benzoyl and Furoyl Isothiocyanates and their Use in Synthesizing Heterocyclic Compounds1, J. Am. Chem. Soc. 56 (3) (1934) 719–721.
[24] S.G. Sadabs, Program for empirical absorption correction of area detector data, University of Göttingen, 1996.
[25] O.D. Rigaku, CrysAlisPro Software System, version 1.171. 38.41 l, , R. Coorporation, Editor. (2015), Oxford, UK.
[26] G.M. Sheldrick, SHELXT–Integrated space-group and crystal-structure determination, Acta Crystallogr. Sect. A: Found. Adv. 71 (1) (2015) 3–8.
[27] G.M. Sheldrick, Crystal structure refinement with SHELXL, Acta Crystallogr. Sect. C: Struct. Chem. 71 (1) (2015) 3–8.
[28] O.V. Dolomanov, et al., OLEX2: a complete structure solution, refinement and analysis program, J. Appl. Crystallogr. 42 (2) (2009) 339–341.
[29] C. Stoe, X-area (version 1.18) and X-red32 (version 1.04). Stoe & Cie, Darmstadt, Germany, 2002.
[30] M.C. Burla, et al., Crystal structure determination and refinement viaSIR2014, J. Appl. Crystallogr. 48 (1) (2015) 306–309.
[31] S. Pektaş, et al., spiro-Cyclotriphosphazenes containing 4-hydroxyphenylethyl pendant arm: Syntheses, structural characterization and DNA interaction study, Inorg. Chim. Acta 474 (2018) 51–65.
[32] J.N. Asegbeloyin, et al., Synthesis, Characterization and in vitro Antibacterial Activity of Co (II), Cu (II) and Ni (II) Complexes with 4-Acylpyrazol-5-one Schiff Bases, Asian J. Chem. 26 (23) (2014).
[33] C. Collins, et al., Estimating microbial numbers, in: Lyne's microbiological methods, 8th ed., Butterworth-Heinemann Ltd, Oxford, 2004, pp. 144–255.
[34] J.N. Asegbeloyin, et al., Synthesis, Characterization, and Biological Activity of N′-[(Z)-(3-Methyl-5-oxo-1-phenyl-1, 5-dihydro-4H-pyrazol-4-ylidene)(phenyl) methyl] benzohydrazide and Its Co (II), Ni (II), and Cu (II) Complexes, Bioinorg. Chem. Appl. 2014 (2014).
[35] Clinical and L.S. Institute, Performance Standards for Antimicrobial Disk Susceptibility Tests for Bacteria Isolated from Animals: CLSI Supplement VET01S; Replaces VET01-S2. 2015: Clinical and Laboratory Standards Institute.
[36] R. Jones, Susceptibility tests: Microdilution and macrodilution broth procedures, Manual Chem. Microbiol. (1985) 972–977.
[37] M.A. Wikler, Methods for dilution antimicrobial susceptibility tests for bacteria that grow aerobically: approved standard, CLSI 26 (2006). M7-A7.
[38] I. Babahan, et al., A novel bidentate ligand containing oxime, hydrazone and indole moieties and its BF2+ bridged transition metal complexes and their efficiency against prostate and breast cancer cells, Appl. Organomet. Chem. (2020), e5632.
[39] I. Babahan, A. Özmen, K. Aslan, Synthesis and use of dioxime ligands for treatment of leukemia and colon cancer cells, Appl. Organomet. Chem. 31 (11) (2017), e3752.
[40] A.C. Ekennia, et al., Synthesis, characterization, molecular docking, biological activity and density functional theory studies of novel 1, 4-naphthoquinone derivatives and Pd (II), Ni (II) and Co (II) complexes, Appl. Organomet. Chem. 32 (5) (2018), e4310.
[41] J.N. Asegbeloyin, et al., Synthesis, Characterization and Antimicrobial Activity of 3-Acetyl-4-hydroxy-6-methyl-(2H) pyran-2-one Schiff Base with 2, 2'-(Ethylenedioxy) diethylamine and its Co (II), Ni (II) and Cu (II) Complexes, Asian J. Chem. 27 (9) (2015).
[42] V. Govindaraj, S. Ramanathan, Synthesis, spectral characterisation, electrochemical, and fluorescence studies of biologically active novel Schiff base complexes derived from E-4-(2-hydroxy-3-methoxybenzlideneamino)-N-(pyrimidin-2-yl) benzenesulfonamide, Turk. J. Chem. 38 (4) (2014) 521–530.
[43] G. Binzet, et al., Nickel (II) and copper (II) complexes of N, N-dialkyl-N′-3-chlorobenzoylthiourea: Synthesis, characterization, crystal structures, Hirshfeld surfaces and antimicrobial activity, J. Mol. Struct. 1161 (2018) 519–529.
[44] E.E. Oyeka, et al., Synthesis, crystal structure, computational analysis and biological properties of 1-(4-chlorobenzoyl)-3-[2-(2-{2-[3-(4-chlorobenzoyl)-thioureido]-ethoxy} ethoxy) ethyl]-thiourea and its Ni (II) and Cu (II) complexes, J. Mol. Struct. 1168 (2018) 153–164.
[45] C.K. Özer, et al., Synthesis and characterization of N-(arylcarbamothioyl)-cyclohexanecarboxamide derivatives: the crystal structure of N-(naphthalen-1-ylcarbamothioyl) cyclohexanecarboxamide, Molecules 14 (2) (2009) 655–666.
[46] G. Binzet, et al., Synthesis, characterization and antimicrobial activities of transition metal complexes of N, N-dialkyl-N′-(2-chlorobenzoyl) thiourea derivatives, J. Coord. Chem. 59 (12) (2006) 1395–1406.
[47] G. Binzet, et al., Synthesis and characterization of novel thiourea derivatives and their nickel and copper complexes, J. Chem. 2013 (2013).
[48] M. Lipowska, et al., Rhenium (V) oxo complexes of novel N2S2 dithiourea (DTU) chelate ligands: Synthesis and structural characterization, Inorg. Chem. 35 (14) (1996) 4227–4231.
[49] E.A.-N. Waheed, Synthesis and characterization of some metals complexes of {N-[(benzoyl amino)-thioxo methyl] proline}, Journal of Science 15 (4) (2012) 1–10.
[50] H. Arslan, et al., Crystal structure and thermal behaviour of copper (II) and zinc (II) complexes with N-pyrrolidine-N′-(2-chloro-benzoyl) thiourea, J. Coord. Chem. 59 (2) (2006) 223–228.
[51] H. Arslan, U. Florke, N. Kulcu, The crystal and molecular structure of 1-(biphenyl-4-carbonyl)-3-p-tolyl-thiourea, Acta Chimica Slovaca 51 (4) (2004) 787–792.
[52] L.C. Ekowo, et al., Synthesis, structure, Hirshfeld surface, DFT and in silico studies of 4-[(E)-(2, 5-dimethoxybenzylidene) amino]-1, 5-dimethyl-2-phenyl-1, 2-dihydro-3H-pyrazol-3-one (DMAP) and its metal complexes, J. Molecul. Struct. (2020) 127994.
[53] O.C. Okpareke, et al., Synthesis, structure, computational and molecular docking studies of asymmetrically di-substituted ureas containing carboxyl and phosphoryl hydrogen bond acceptor functional groups, J. Mol. Struct. 1203 (2020), 127360.
[54] A.G. Doyle, E.N. Jacobsen, Small-molecule H-bond donors in asymmetric catalysis, Chem. Rev. 107 (12) (2007) 5713–5743.
[55] P. Gale, S. Garc, A. Garrido, J. Garric, Chem. Soc. Rev. 37 (2008) 151–190.
[56] G. Binzet, et al., cis-Bis [N′-(4-bromobenzoyl)-N, N-dimethylthioureato-κ2O, S] copper (II), Acta Crystallogr. Sect. E: Struct. Rep. Online 67 (5) (2011) m648–m649.
[57] G. Binzet, et al., Synthesis and characterization of Cu (II) and Ni (II) complexes of some 4-bromo-N-(di (alkyl/aryl) carbamothioyl) benzamide derivatives, J. Coord. Chem. 62 (21) (2009) 3454–3462.
[58] S.Y. Wu, et al., Synthesis and Characterization of N, N-Di-substituted Acylthiourea Copper (II) Complexes, Z. Anorg. Allg. Chem. 641 (5) (2015) 883–889.
[59] K.R. Koch, New chemistry with old ligands: N-alkyl-and N, N-dialkyl-N′-acyl (aroyl) thioureas in co-ordination, analytical and process chemistry of the platinum group metals, Coord. Chem. Rev. 216 (2001) 473–488.
[60] H.A. Nkabyo, et al., Understanding the mechanism of cis–trans isomerism in photo-active palladium (II) complexes derived from the N, *N-di-substituted benzoylthioureas*, Inorganica Chimica Acta 512 (2020), 119884.
[61] J. Coetzer, J. Boeyens, Crystal and molecular structure of bis (2, 2, 6, 6-tetramethylheptane-5-thiolo-3-onato) nickel (II), J. Crystal Mol. Struct. 1 (4) (1971) 277–283.

[62] P. Knuuttila, et al., The Crystal and Molecular Structure of Bis (l, l-diethyl-3-benzoyl-thioureato) nickel (II), Acta Chem. Scandinavia A 36 (6) (1982) 541–545.
[63] B. Lorenz, et al., *Koordinationsverbindungen des 2-Hydroxy-4, 6-diphenyl-thiobenzophenons. Chelat-Komplexe des Cobalts und Nickels, Röntgenkristallstrukturanalyse der Nickelverbindung*, Zeitschrift für anorganische und allgemeine Chemie 619 (1993) 111905–111908.
[64] S. Sawusch, et al., Templat-Reaktionen von 3, 5-Diphenyl-1, 2-dithioliumchlorid mit (Thio) Benzoylhydrazin sowie Nickel-und Zinkacetat/Template Reactions of 3.5-Diphenyl-1.2-dithiolium Chloride with (Thio) Benzoylhydrazine and Nickel or Zinc Acetate, Zeitschrift für Naturforschung B 52 (9) (1997) 1139–1142.
[65] U. Schröder, et al., Ligand Properties of N-Acyl-thiocarbamic-O-alkylesters–A new class of aza-analogous 1, 3-thioxoketones, J. für Praktische Chemie/Chemiker-Zeitung 337 (1) (1995) 184–188.
[66] O. Siiman, et al., Single-crystal structure and 5.0. deg. K polarized electronic spectra of bis (monothioacetylacetonato) nickel (II). Far-infrared and Raman spectra of bis (monothioacetylacetonato) metal (II) complexes, J. Am. Chem. Soc. 96 (8) (1974) 2353–2359.
[67] B. Tweedy, Possible mechanism for reduction of elemental sulfur by monilinia fructicola. in Phytopathology. 1964. AMER Phytopathological Soc 3340 Pilot Knob Road, St Paul, MN 55121.
[68] A.A. Hassan, et al., Design, synthesis, and DNA interaction studies of furo-imidazo [3.3. 3] propellane derivatives: Potential anticancer agents, Bioorg. Chem. 85 (2019) 585–599.
[69] B. Abulhasanov et al., Synthesis, characterization, duplex-DNA interactions, and anticancer activities of novel octahedral [Ni (phen) 2 (dppz-idzo)] 2+ and [Co (phen) 2 (dppz-idzo)] 3+ complexes. Applied Organometallic Chemistry: p. e5866.
[70] B. Atabey-Ozdemir, et al., Cytotoxicity and DNA binding of copper (II) and zinc (II) complexes of flavonoids: quercitrin, myricitrin, rutin, Bul. Chem. Commun. 49 (4) (2017) 901–907.
[71] B. Coban, N. Eser, I. Babahan, DNA binding by copper (II) complexes of semithiocarbazone containing ligands, Interactions 5 (11) (2017) 12.
[72] B. Coban, et al., DNA studies of newly synthesized heteroleptic platinum (II) complexes [Pt (bpy)(iip)] 2+ and [Pt (bpy)(miip)] 2+, J. Biol. Inorg. Chem. 21 (2) (2016) 163–175.
[73] B. Coban, U. Yildiz, DNA-binding studies and antitumor evaluation of novel water soluble organic pip and hpip analogs, Appl. Biochem. 172 (1) (2014) 248–262.
[74] M.M. Kasprzak, A. Erxleben, J. Ochocki, Properties and applications of flavonoid metal complexes, RSC Adv. 5 (57) (2015) 45853–45877.
[75] O.D. Okagu, et al., Synthesis and characterization of Cu (II), Co (II) and Ni (II) complexes of a benzohydrazone derivative: Spectroscopic, DFT, antipathogenic and DNA binding studies, J. Mol. Struct. 1183 (2019) 107–117.
[76] U. Yildiz, B. Coban, Chemical and photo-induced nuclease activity of a novel minor groove DNA binder Cu (II) complex, J. Serb. Chem. Soc. 84 (6) (2019) 563–574.
[77] C.S. Devi, et al., Recent Advances in Copper Intercalators as Anticancer Agents, J. Fluoresc. 28 (5) (2018) 1195–1205.
[78] Y. Kobayashi, et al., Direct N-glycofunctionalization of amides with glycosyl trichloroacetimidate by thiourea/halogen bond donor co-catalysis, Angew. Chem. Int. Ed. 57 (14) (2018) 3646–3650.
[79] S. Selvaraj, et al., Flavonoid–metal ion complexes: a novel class of therapeutic agents, Med. Res. Rev. 34 (4) (2014) 677–702.
[80] K. Poole, Mechanisms of bacterial biocide and antibiotic resistance, J. Appl. Microbiol. 92 (2002) 55S–64S.
[81] K. Todar, Bacterial resistance to antibiotics (page 3). Todar's online textbook of bacteriology; 2011: p. 4.
[82] H. Nikaido, Prevention of drug access to bacterial targets: permeability barriers and active efflux, Science 264 (5157) (1994) 382–388.
[83] A. Boags, et al., Progress in molecular dynamics simulations of Gram-negative bacterial cell envelopes, J. Phys. Chem. Lett. 8 (11) (2017) 2513–2518.
[84] M. Mitra, et al., Distinct intramolecular hydrogen bonding dictates antimicrobial action of membrane-targeting amphiphiles, J. Phys. Chem. Lett. 10 (4) (2019) 754–760.
[85] H. Arslan, et al., Antimicrobial activity of some thiourea derivatives and their nickel and copper complexes, Molecules 14 (1) (2009) 519–527.
[86] S.S. Bhat, et al., Synthesis, electronic structure, DNA and protein binding, DNA cleavage, and anticancer activity of fluorophore-labeled copper (II) complexes, Inorg. Chem. 50 (2) (2011) 545–558.
[87] C. Santini, et al., Advances in copper complexes as anticancer agents, Chem. Rev. 114 (1) (2014) 815–862.